HiSST: 2nd International Conference on
High-Speed Vehicle Science Technology
11–15 September 2022, Bruges, Belgium

Simulating Hypersonic Fluid Structural Interaction of an Inclined Cantilever Panel Using the Conservation Element Solution Element Method

L. Pollock[1], G. Wild[2]

Abstract

This manuscript presents the simulation of the Fluid Structural Interaction (FSI) of a cantilever compliant panel in hypersonic flow. The problem is resolved through multiphysics coupling in the commercial software package LS-DYNA and employs the use of the Immersed Boundary Method (IBM) within the Conservation Element Solution Element (CESE) solver framework using explicit time stepping. The CESE method encompasses many non-traditional features that makes it aptly suited for the study of hypersonic flows, including, a unified treatment of space and time, and a Riemann-free shock solver. The study of hypersonic FSI is of high importance due to restrictive weight requirements resulting in thin panels that are prone to deformation. The understanding of the aeroelastic effects is important to ensure continued operation of geometry sensitive regions such as inlets and control surfaces.

Keywords: *Conservation Element Solution Element, Fluid Structural Interaction, Immersed Boundary Method, hypersonic, aeroelastic*

1. Introduction

The study of Hypersonic Vehicles (HSVs) has experienced exponential growth in recent decades, largely owing to increased security concerns related to the military application of such vehicles [1]. Unlike the distinction between subsonic and supersonic flows, hypersonic flight does not exhibit such a stark change in physics but is typically defined by the onset of one or more features including, thin shock layers, entropy layers, viscous interactions, chemically reacting flows, and low-density flows [2, 3]. Due to the complexity and variety of phenomena, a typical use of flow in excess of Mach 5 is applied to characterize the onset of hypersonic conditions. However, this definition is not standardized and in some cases the onset of hypersonics has been applied to flows as low as Mach 3 or as large as Mach 7 [2].

Computational tools are widely applied for the study of hypersonic flows because of two main reasons. Firstly, the coupled and complex fluid phenomena at these high velocities yields traditional analytical solutions invalid, and numerical schemes must be adopted. Secondly, ground test facilities are limited in their ability to recreate the necessary conditions for hypersonic flow and scientific launch vehicles remain costly to produce. As such, large efforts have been undertaken for the development and validation of both high- and low-fidelity computational models to study the underpinning fluid dynamics. Even greater complexity is introduced when it is necessary to study the multiphysics coupling of structural, thermal, and fluid dynamics. The effects of aerodynamic deformation or aeroelasticity becomes more pronounced in HSVs partially because of the high thermal loads and reduced material stiffness but also because of the stringent design requirements for the vehicles that limits the use of

[1] *UNSW Canberra, 1 Northcott Drive, Campbell, ACT, 2620, Australia, L.Pollock@adfa.edu.au*

[2] *UNSW Canberra, 1 Northcott Drive, Campbell, ACT, 2620, Australia, G.Wild@adfa.edu.au*

structural stiffening [4]. Hence, HSVs typically operate close to their maximum design envelope where aeroelastic effects may have devastating consequences. A thorough understanding of the Fluid Structural Interaction (FSI) yields a reduction in vehicle uncertainty and improved reliability.

A variety of computational tools, both experimental and commercial have been applied for the study of hypersonic FSI. These tools range in their complexity from inviscid solutions, sometimes called panel codes, which are typically applied for preliminary design analysis through to direct numerical simulation (DNS) which aims to resolve all turbulent eddies within the Kolmogorov scales, both spatial and temporal [5]. DNS still largely exceeds the computational power of modern computing systems, especially for hypersonic flows as the number of computational operations grows on the order of Reynold's number to the third power (Re^3). Hence, DNS remains largely experimental and is often employed for the development and study of turbulence closure models.

The Hypersonics Research Group at the University of New South Wales Canberra has an ongoing research program into hypersonic fluid-thermal-structural interaction (FTSI). In this work, a previous experimental case [6] is re-examined using an emerging computational fluid dynamics (CFD) method.

2. Background

2.1. LS-DYNA

In this study, the commercial software package LS-DYNA is used. First developed by the Livermore Software Technology Company in 1976 for the simulation of low altitude release weaponry, the software has been developed to handle highly non-linear, transient events. LS-DYNA was acquired by ANSYS Inc. in 2019 and is slowly being incorporated into their existing platform [7]. In recent years, a novel CFD package has been implemented in LS-DYNA to extend the software's multiphysics capability and is in line with the original purpose of the software, to study highly non-linear, transient, high-energy events.

2.2. The Conservation Element Solution Element Method

The novel Conservation Element Solution Element (CESE) method has not been broadly applied to the study of hypersonic flows but presents with many favourable properties, including a Reimann-free shock solver which greatly improves the ability to capture shock waves [8]. Ultimately, this research aims to explore the CESE method for the study of hypersonic FSI to inform the computational community and guide potential research in the field. The CESE method was developed by Chang [9] at the NASA Glenn Research Centre in the early 1990s with ongoing work at the NASA Langley research centre on the *ez4d* code towards the development of an unstructured, compressible, CESE scheme with Reynold's Averaged Navier Stokes (RANS) turbulence modelling [10]. The CESE method is a special variant of the finite-volume discretization method that is applied for the solution of the conservation laws. A brief presentation of the CESE method adapted from Wang [11] is given below. A detailed discussion of the CESE method is not the focus of this work and readers are directed to Jiang, et al. [12] and Chang [10] for more detail.

We begin by considering the 3-dimensional Euler equations in conservation form but are not limited to such applications. For the following, ρ denotes the fluid density, u, v, and w, the x-, y-, and z-, fluid velocity components, respectively, P is the pressure, and e is the total energy per unit mass.

$$\frac{\partial \boldsymbol{Z}}{\partial t} + \frac{\partial \boldsymbol{L}}{\partial x} + \frac{\partial \boldsymbol{M}}{\partial y} + \frac{\partial \boldsymbol{N}}{\partial z} = 0 \tag{1}$$

Where $\boldsymbol{Z}$ is the vector of conservation variables defined by,

$$\boldsymbol{Z} = \begin{bmatrix} \rho \\ \rho u \\ \rho v \\ \rho w \\ \rho e \end{bmatrix} \tag{2}$$

And $\boldsymbol{L}$, $\boldsymbol{M}$, $\boldsymbol{N}$, are the x-, y-, and z- inviscid flux vectors, respectively, defined by,

$$\boldsymbol{L} = \begin{bmatrix} \rho u \\ \rho u^2 + P \\ \rho uv \\ \rho uw \\ (\rho e + P)u \end{bmatrix}, \qquad \boldsymbol{M} = \begin{bmatrix} \rho v \\ \rho vu \\ \rho v^2 + P \\ \rho vw \\ (\rho e + P)v \end{bmatrix}, \qquad \boldsymbol{N} = \begin{bmatrix} \rho w \\ \rho wu \\ \rho wv \\ \rho w^2 + P \\ (\rho e + P)w \end{bmatrix} \tag{3}$$

The integral form of the previous equations for a finite control volume V is then given by,

$$\iiint_V \left(\frac{\partial \boldsymbol{Z}}{\partial t} + \frac{\partial \boldsymbol{L}}{\partial x} + \frac{\partial \boldsymbol{M}}{\partial y} + \frac{\partial \boldsymbol{N}}{\partial z} \right) dV = 0 \tag{4}$$

Defining $\boldsymbol{h}$ as $[\boldsymbol{L} \quad \boldsymbol{M} \quad \boldsymbol{M} \quad \boldsymbol{U}]$, Eq. (4) becomes,

$$\iiint_V (\nabla \cdot \boldsymbol{h})\, dV = 0 \tag{5}$$

Equation (5) represents a finite control volume, V, that is unified in space and time and where ∇ is the vector operator $\left[\frac{\partial}{\partial x} \quad \frac{\partial}{\partial y} \quad \frac{\partial}{\partial z} \quad \frac{\partial}{\partial t}\right]$. Application of Gauss' theorem to Eq. (5) allows for the volume integral to be converted to the surface integral,

$$\oint_{s(V)} \boldsymbol{h} \cdot d\boldsymbol{s} = 0 \tag{6}$$

Equation (6) is the overarching focus of the CESE method of which discretization is applied. Implementation of the CESE method involves the creation of two different types of elements, the Conservation Element (CE) and the Solution Element (SE) from which the method derives its name [13]. In each CE the conservation laws are enforced whilst in the SE the flow variables are approximated by a function, typically a first order Taylor series expansion. In the CESE method, the derivatives of the transported properties are solved directly and not approximated by the properties themselves.

The CESE setup is illustrated in Fig 1 below, here the CE for the centre element is defined at the centroid of the region A-B-C-D whereas the SE is defined relative to the centroid of the region CE_1-A-CE_2-B-CE_3-C-CE_4-D, hence, the centroid location of the CE and SE do not necessarily coincide which can result in instabilities for highly skewed meshes such as those utilized in boundary layers. The simplest 2D mesh is composed of triangular elements and is hence, well suited for use in unstructured solvers. However, the method has been extended to handle general shaped polygons [14].

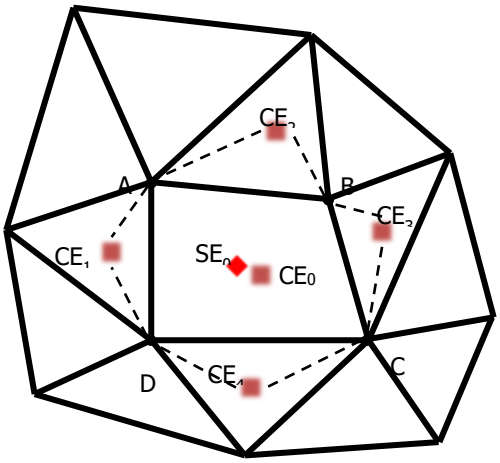

Fig 1. An illustration of the CE/SE schematic.

The integral form of the conservation laws that has been derived is fundamentally a second-order accurate method which is central winding and non-dissipative in both time and space with flux conservation guaranteed. The original explicit scheme is only conditionally dependent upon the Courant-Friedrich-Lewy criterion. Work has also been completed towards a fourth-order accurate method [15, 16].

Further work has been completed to add artificial dissipation to the original scheme to allow for modelling of real physical phenomena. The resulting scheme, named a-α-β-ε, weights the spatial derivatives based on the differences between the central difference and non-dissipative components (the ε term) as well as the difference between the upwind component and the central difference component (the β term). Where the upwind component is calculated as a ratio of weighted upstream and downstream variables (the α term).

$$\boldsymbol{Z} = \boldsymbol{Z}^{\alpha} + 2\varepsilon(\boldsymbol{Z}^{C} - \boldsymbol{Z}^{\alpha}) + \beta(\boldsymbol{Z}^{w} - \boldsymbol{Z}^{c}) \tag{7}$$

$$\boldsymbol{Z}^{w} = \frac{|x_{+}|^{\alpha} x_{-} + |x_{-}|^{\alpha} x_{+}}{|x_{+}|^{\alpha} + |x_{-}|^{\alpha}} \tag{8}$$

The a-α-β-ε method suppresses oscillations near discontinuities and is controlled through empirically determined values which can be adapted locally to the flow conditions. Thus far, the method has been applied to solve magnetohydrodynamics [17], chemically reacting flows [18], multiphase flows [19], detonations [20], and aeroacoustics [21]. The primary advantages for hypersonic flows include:

- Reimann-free shock solver
- Excellent shock capturing
- Excellent at handling stiff terms
- Faster than conventional finite volume method (FVM)
- Easy treatment of boundary conditions (including non-reflecting)

The CESE solver within LS-DYNA does not implement any turbulence modelling due to the difficulty of adapting a loosely conservative wall model with the strongly conservative CESE scheme. Hence, whilst only laminar flows can be solved with great confidence their dominance in hypersonic flows still provides good agreement with experimental observations. Furthermore, due to the inherent non-dissipative nature of the CESE α scheme, there exists the possibility of including artificial viscous dissipation to generate an Implicit Large Eddy Simulation (ILES) [11, 22]. In ILES, the mesh is refined enough to capture large eddies whilst the artificial viscous dissipation acts as a sub-grid scale turbulence model, resolving the effects of the high frequency turbulence components. As such, implicit turbulence modelling remains possible but difficult.

2.3. The Immersed Boundary Method

Within the CESE solver of LS-DYNA there exists two different FSI coupling methods, the Immersed Boundary Method (IBM), as introduced by Peskin [23] for the study of blood flow through a beating heart, and the Moving Mesh (MM) method [24]. In both cases, the fluid forces (pressures) are passed to the structural solver from which displacements and velocities are passed back to the fluid solver using weak coupling. The MM method is the most common FSI coupling technique due to its high accuracy and boundary layer capture. Whilst effective, the MM method is prone to instabilities, especially at large deformations, requiring the careful tuning of control parameters. At each time step, the fluid mesh is updated using any number of techniques, often through iterative means and predictor-corrector methods to resolve the accurate location of the new mesh. The MM method is more accurate than IBM but at higher computational expense. As an alternative, the IBM method employs Eulerian mesh that is fixed in time and space. In LS-DYNA the direct forcing and ghost fluid methods are employed with the no-slip condition enforced at the FSI boundary using a Lagrangian structural mesh [24-26]. The IBM method overcomes the numerical stiffness often encountered with various MM techniques and is naturally more stable due to the lack of dynamic mesh updates. As such, the IBM method is typically easier to employ without the need for fine-tuning of stability parameters and can be utilized for the simulation of free flight or six Degree of Freedom (6DOF) dynamics.

3. Sod's Shock Tube

Before progressing to the FSI case, a 1-dimensional version of the CESE method was implemented in MATLAB to solve the Sod's shock tube problem. The development of the 1D code allows for an improved understanding of the underlying mechanics as well as validation to a canonical flow problem with a known analytical solution. Moreover, the 1D code presents as the first step towards a larger project – to develop an in-house CESE code. The results of this 1D code, as shown in Fig 2 and Fig 3 show good agreement with the analytical solution. A sparse solution with 2^4 elements does not resolve the fine features of the problem, as expected, but captures the general behavior. A comparison is also presented between cases with and without artificial dissipation to shown that numerical overshoots can be adequately suppressed. The solution with artificial dissipation is referred to as the damped solution.

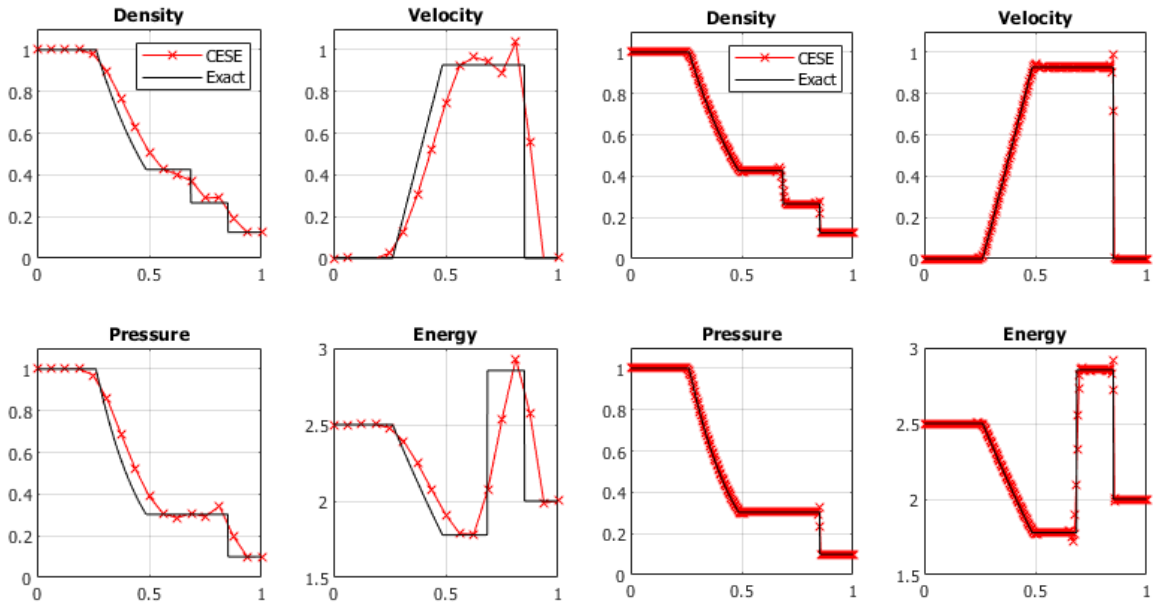

Fig 2. A comparison between undamped Sod's shock tube solutions for 2^4 (left) and 2^8 (right) elements.

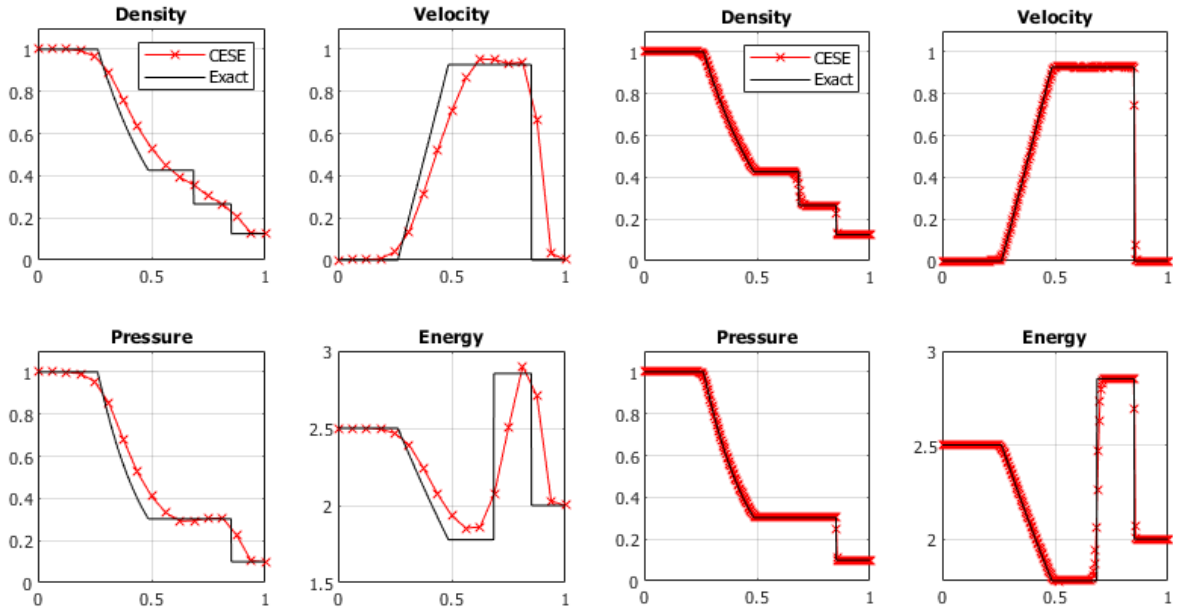

Fig 3. A comparison between damped Sod's shock tube solutions for 2^4 (left) and 2^8 (right) elements.

Figure 5 below compares undamped and damped solutions at the 85% shockwave. As shown, the damped solution performs exceptionally well to suppress the numerical overshoots which arise from the inherently small dissipation in the scheme which sacrificing accuracy.

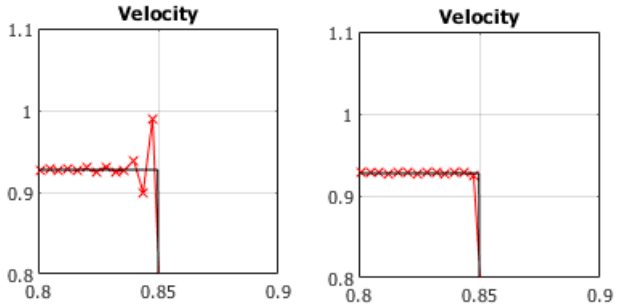

Fig 4. A comparison between undamped (left) and damped (right) Sod's shock tube solutions.

The results of the 1D code show great promise for the CESE scheme. The scheme is conservative, efficient, and can accurately capture shocks without the use of a Riemann solver. The natural lack of dissipation means that a tailored shock-capturing method can also be developed to suit specific requirements.

4. Setup and Results

The FSI test case is composed of an inclined cantilever structure and has been previously studied experimentally by Currao, et al. [6] under the name HyFoil. The structure comprises both compliant and rigid support sections. The compliant panel is composed of aluminium 6061-T6 with a nominal thickness of 2 mm, length of 130 mm and width of 80 mm. The rigid support is 100 mm long and 10 mm thick, inclined at a 20-degree angle with a leading-edge wedge angle of 45 degrees. The use of the preceding support structure and uniform geometry minimises 3-dimensional effects and as such,

the problem has only been studied here 2-dimensionally. A sketch of the geometry is shown in Fig 5 below with compliant panel properties summarised in Table 1 as used by [6].

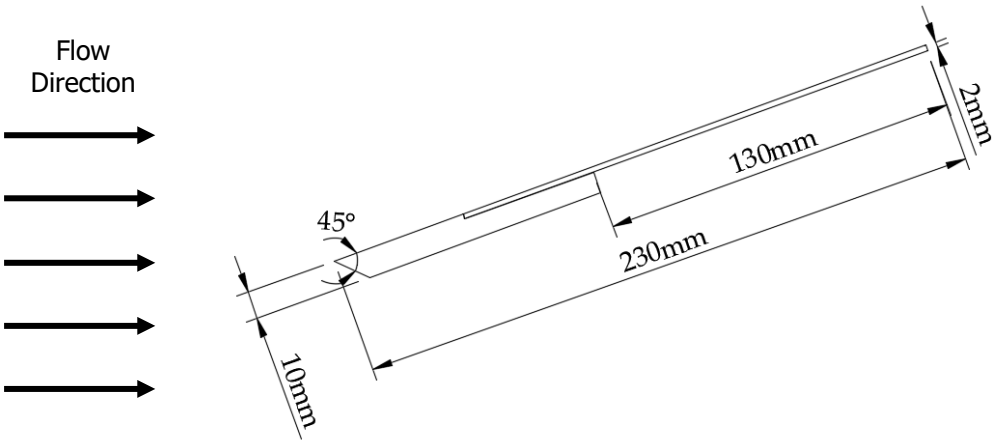

Fig 5. A sketch of the geometry.

Table 1. The properties of the compliant panel.

Length (mm)	Width (mm)	Thickness (mm)	Young's Modulus (GPa)	Density (kg/m^3)	Damping Ratio
130 (±0.1)	80 (±0.1)	1.95 (±0.1)	52.7 (±0.1)	2668 (±0.1)	0.0038

The case was experimentally tested using a free-piston driven compression-heated Ludwieg tube at the University of Southern Queensland facility, hereafter referred to as TUSQ. The case is for a Mach 5.85 flow with freestream Reynold's number of $7.16 \cdot 10^6$ m^{-1}. The flow conditions are summarised in Table 2.

Table 2. A summary of the test flow conditions.

Freestream Mach	Freestream Pressure (Pa)	Freestream Temperature (K)	Freestream Density (kg/m^3)	Wall Temperature (K)	Reynold's Number (m^{-1})
5.85	755	75	0.0351	290	7.16 x 10^6

The case was implemented numerically in LS-DYNA using a prescribed inlet on the left-hand side edge and non-reflecting boundaries (NRBC) on the remaining three edges. The NRBCs are uniquely easy to implement under the CESE scheme and are exceptional at preventing any weak reflected shocks from re-entering the domain. Because of this, the CESE method has dominantly been implemented for the study of compressible aeroacoustics.

Initial results from the simulation indicate good agreement with both the experimental and FVM methods. The agreement between the CESE method and experiment diverges as the flow time increases which may be the result of three main factors.

Firstly, determination of the correct flow damping parameters (α, β, ε). Work has not been undertaken to examine the effects of damping parameters in various flow regimes. Thus far, these damping parameters must be determined empirically, with little quantitative methods to calculate them. Future work on the CESE method could be towards modelling the damping parameters (either locally or globally), akin to turbulence closure modelling. Alternatively, different approaches could be explored for adding numerical dissipation to the scheme.

Secondly, the use of the IBM which reduces the fidelity of the near-wall region. Whilst the IBM offers many advantages, including the ability to capture large deflections and decreased computational expenses due to no requirement to remesh, the technique does not accurately capture the near wall mechanics. Whilst the cantilever case is largely driven by inviscid forces, capturing the boundary layer and accompanying phenomena remains an important feature to resolve.

Thirdly, a mesh indepdence study has not yet been undertaken for this case. The initial goal of this work was to first determine whether the CESE method could accurately model hypersonic flow and further, hypersonic FSI, before proceeding into more detailed analysis.

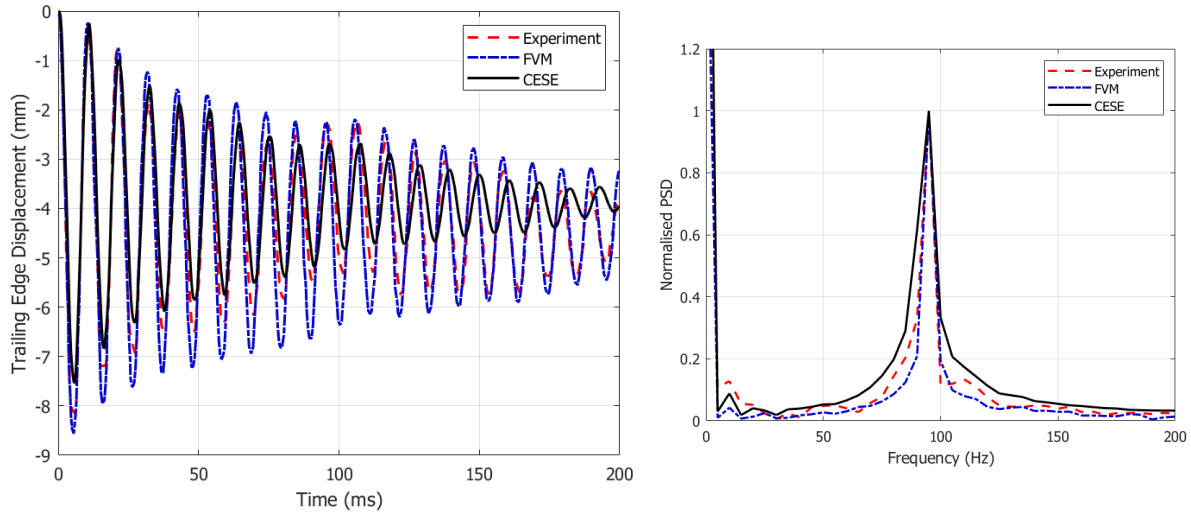

Fig 6. Results comparison showcasing trailing edge displacement (left) and its spectrum (right).

Despite its shortcomings, mainly due to a lack of research and development, the CESE scheme along with the IBM prove to be much less computationally expensive than other FVM counterparts. Such a case presented here could typically take on the order of 8 – 50 days to simulate using a conventional implicit FVM approach with 25 computational cores. The explicit CESE results presented here can be obtained between 2 – 4 days, depending on the detail of the mesh. Hence, the CESE method, even at this level of development, presents with great potential for the study of hypersonic FSI.

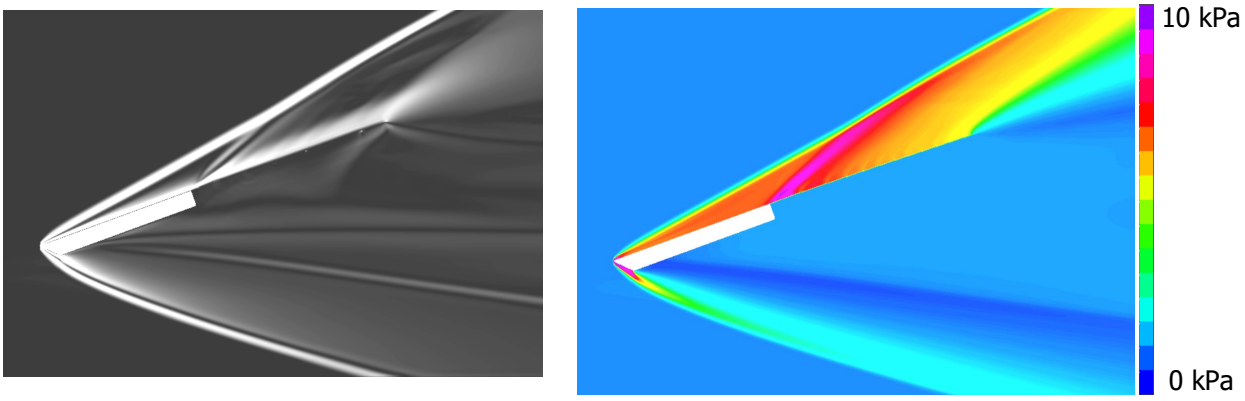

Fig 7. CESE results showcasing numerical schlieren (left) and static pressure (right) contours.

Finally, Figure 8 provides a comparison between numerical schlieren and static pressure contours. Many of the flow features have been adequately captured, including the leading-edge shock and trailing edge expansion fan.

5. Conclusion

This work has explored the use of the Conservation Element Solution Element scheme along with the Immersed Boundary Method implemented in the commercial software LS-DYNA for the study of hypersonic fluid structural interaction. The new results have been compared with a previous study undertaken by [6]. Whilst there is potential to further refine the solution, the results presented reveals reasonable agreement with both the experimental and FVM cases and is obtained in much shorter time. Ultimately, the CESE scheme presents as a useful tool for the study of hypersonic fluid dynamics with plenty of potential for greater improvement. Thus far, the CESE scheme implemented in LS-DYNA has not been fully supported as an aerodynamic CFD package and has mainly been used for the implementation of multiphysics support. The development of an in-house or open source CESE code would allow for the tailoring of the scheme to hypersonic fluid dynamics, including the implementation of turbulence modelling.

References

1. R. H. Speier, G. Nacouzi, C. Lee, and R. M. Moore, Hypersonic missile nonproliferation: hindering the spread of a new class of weapons. Rand Corporation, 2017.
2. J. D. Anderson, Hypersonic and high temperature gas dynamics. AIAA, 2000.
3. L. Pollock and G. Wild, An initial review of hypersonic vehicle accidents, in 19th Australian International Aerospace Congress, Melbourne, Australia, 2021.
4. L. Pollock and G. Wild, Modal Analysis of a Scramjet Inlet for Optimization of Sensor Placement, in ASCEND 2021, 2021: American Institute of Aeronautics and Astronautics, in ASCEND, doi: doi:10.2514/6.2021-4084
   10.2514/6.2021-4084. [Online]. Available: https://doi.org/10.2514/6.2021-4084
5. P. Moin and K. Mahesh, Direct numerical simulation: a tool in turbulence research, Annual review of fluid mechanics, vol. 30, no. 1, pp. 539-578, 1998.
6. G. M. Currao, A. J. Neely, D. R. Buttsworth, and S. L. Gai, Hypersonic fluid-structure interaction on a cantilevered plate, research and development, vol. 12, p. 13, 2017.
7. L. Pollock, N. North, and G. Wild, Explicit Dynamic Finite Element Simulation of Plate Impacts for Damage Localisation.
8. S.-T. Yu, S.-C. Chang, S.-T. Yu, and S.-C. Chang, Treatments of stiff source terms in conservation laws by the method of space-time conservation element/solution element, in 35th Aerospace Sciences Meeting and Exhibit, 1997, p. 435.
9. S.-C. Chang, A new numerical framework for solving conservation laws: the method of space-time conservation element and solution element. National Aeronautics and Space Administration, 1991.
10. C.-L. Chang, Time-accurate, unstructured mesh Navier-Stokes computations with the CESE method, in 42nd AIAA/ASME/SAE/ASEE Joint Propulsion Conference & Exhibit, 2006, p. 4780.
11. X.-Y. Wang, A summary of the space-time conservation element and solution element (CESE) method. National Aeronautics and Space Administration, Glenn Research Center, 2015.
12. Y. Jiang, C.-Y. Wen, and D. Zhang, Space–Time Conservation Element and Solution Element Method and Its Applications, AIAA Journal, vol. 58, no. 12, pp. 5408-5430, 2020.
13. Z.-c. Zhang, G. Cook Jr, and K.-s. Im, Overview of the CESE Compressible Fluid and FSI Solvers.
14. B. S. Venkatachari, G. Cheng, and S.-C. Chang, Validation and Verification of CE/SE Method Based Courant Number Insensitive Transient Viscous Flow Solver, in 41st AIAA/ASME/SAE/ASEE Joint Propulsion Conference & Exhibit, 2005, p. 4356.
15. D. L. Bilyeu, S.-T. J. Yu, Y.-Y. Chen, and J.-L. Cambier, A two-dimensional fourth-order unstructured-meshed Euler solver based on the CESE method, Journal of Computational Physics, vol. 257, pp. 981-999, 2014.
16. C.-L. Chang, B. S. Venkatachari, and G. Cheng, Time-accurate local time stepping and high-order space time CESE methods for multi-dimensional flows using unstructured meshes, in 21st AIAA Computational Fluid Dynamics Conference, 2013, p. 3069.

17. M. Zhang, S.-T. J. Yu, S.-C. H. Lin, S.-C. Chang, and I. Blankson, Solving the MHD equations by the space–time conservation element and solution element method, Journal of Computational Physics, vol. 214, no. 2, pp. 599-617, 2006.
18. S.-T. Yu, S.-C. Chang, S.-T. Yu, and S.-C. Chang, Applications of the space-time conservation element/solution element method to unsteady chemically reacting flows, in 13th Computational Fluid Dynamics Conference, 1997, p. 2099.
19. R. Danish Aslam, A. Ali, A. Rehman, and S. Qamar, The space-time conservation element and solution element scheme for simulating two-phase flow in pipes, Advances in Mechanical Engineering, vol. 11, no. 12, p. 1687814019898359, 2019.
20. S. Yu, S.-C. Chang, and P. Jorgenson, Direct calculation of detonation with multi-step finite-rate chemistry by the space-time conservation element and solution element method, in 30th Fluid Dynamics Conference, 1999, p. 3772.
21. C.-K. Kim, S.-T. J. Yu, and Z.-C. Zhang, Cavity Flows in a Scramjet Engine by the Space-Time Conservation and Solution Element Method, AIAA journal, vol. 42, no. 5, pp. 912-919, 2004.
22. L. G. Margolin, W. J. Rider, and F. F. Grinstein, Modeling turbulent flow with implicit LES, Journal of Turbulence, no. 7, p. N15, 2006.
23. C. S. Peskin, Numerical analysis of blood flow in the heart, Journal of computational physics, vol. 25, no. 3, pp. 220-252, 1977.
24. G. Cook, Z.-C. Zhang, and K.-s. Im, Applications of the CESE method in LS-DYNA, in 21st AIAA Computational Fluid Dynamics Conference, 2013, p. 3070.
25. R. P. Fedkiw, T. Aslam, B. Merriman, and S. Osher, A non-oscillatory Eulerian approach to interfaces in multimaterial flows (the ghost fluid method), Journal of computational physics, vol. 152, no. 2, pp. 457-492, 1999.
26. J. Mohd-Yusof, Combined immersed-boundary/B-spline methods for simulations of flow in complex geometries, Center for turbulence research annual research briefs, vol. 161, no. 1, pp. 317-327, 1997.